

Effect of 1 wt% CoO addition on dielectric and microstructural behaviour of $(\text{SrO} \cdot \text{TiO}_2) - (2\text{SiO}_2 \cdot \text{B}_2\text{O}_3)$ glass and glass ceramic[†]

O P THAKUR, DEVENDRA KUMAR, OM PARKASH* and LAKSHMAN PANDEY**

Department of Ceramic Engineering, *School of Materials Science and Technology, Institute of Technology, Banaras Hindu University, Varanasi 221 005, India

**Department of Post Graduate Studies and Research in Physics, Rani Durgavati Vishwavidyalaya, Jabalpur 482 001, India

Abstract. Glass of the nominal composition 64 wt% $(\text{SrO} \cdot \text{TiO}_2)$ –35 wt% $(2\text{SiO}_2 \cdot \text{B}_2\text{O}_3)$ –1 wt% (CoO) was prepared. The glass samples were subjected to heat treatment at 900 and 950 °C. The phase progression in these glass ceramics from X-ray diffraction studies shows the formation of $\text{Sr}_2\text{B}_2\text{O}_5$ as primary crystalline phase followed by rutile (TiO_2), $\text{Sr}_3\text{Ti}_2\text{O}_7$, $\text{SrB}_2\text{Si}_2\text{O}_8$ and $\text{Sr}_3\text{B}_2\text{SiO}_8$ as secondary phases. The first DTA exothermic peak of glass corresponds to the crystallization of $\text{Sr}_2\text{B}_2\text{O}_5$, rutile and $\text{Sr}_3\text{Ti}_2\text{O}_7$ phase while second crystallization peak may be assigned to the formation of $\text{SrB}_2\text{Si}_2\text{O}_8$ and $\text{Sr}_3\text{B}_2\text{SiO}_8$ phases. From microstructure studies we find that strontium borate grows with larger grain size whereas the other phases like $\text{Sr}_3\text{Ti}_2\text{O}_7$, TiO_2 appear smaller in size. Cobalt oxide content in the strontium titanate borosilicate glass ceramic gives the thermal stability to dielectric behaviour and decreases the dielectric loss.

Keywords. Glass ceramics; microstructure; crystallization.

1. Introduction

Because of the immense scope of glass ceramics several workers (Hirayama and Subbarao 1962; Bergeron and Russell 1965; Borelli 1967; Orlova 1969; Mel' nichchenko 1970; Lynch and Shelby 1984) have been attempting to produce glass ceramics having high permittivity, low dielectric loss, high electrical resistance and breakdown strength. Preparation of glass ceramics consists of first making a homogeneous glass in the desired form and subjecting it to controlled crystallization to produce homogeneous micro-crystalline product. These objects are free from pores in contrast to traditionally sintered ceramics (McMillan 1979).

A very little work has been carried out on strontium titanate glass ceramic system despite its wide applications (Lawless 1971, 1974). A detailed investigation of strontium titanate aluminosilicate glass ceramics on dielectric properties and crystallization behaviour shows the effect of purity of starting material and nucleation treatment (Swartz 1985; Swartz and Bhalla 1986; Swartz *et al* 1988).

The crystallization behaviour and dielectric properties of strontium titanate borosilicate glass ceramics have been recently investigated (Thakur *et al* 1995a). These studies have shown that both the glass composition and heat treatment conditions determine the crystalline phase constitution and thus the dielectric properties of corresponding glass ceramics. It is reported that (Thakur *et al* 1993) the addition of bismuth oxide in strontium titanate borosilicate glass ceramic system affects significantly their crystallization, microstructure and hence dielectric behaviour.

[†]Paper presented at the poster session of MRSI AGM VI, Kharagpur, 1995

In the present paper we aim to present investigations on the influence of 1 wt% CoO addition in parent glass towards their crystallization, microstructure and dielectric behaviour.

2. Experimental

Compounds with purity better than 99% of each constituent were used for preparation of glass. A proportionate well mixed batch contained in a high alumina crucible was heated up to 1523 K and held for one hour for better homogenization. The melt was casted in an aluminium mould and annealed at 673 K for 2 h. Subsequently the furnace was turned off, thus the glass specimens were cooled naturally in the furnace. X-ray diffraction was used to confirm the amorphous nature of glass specimens. Infrared spectra for powdered specimen in the form of pellets were recorded in $400\text{--}3600\text{ cm}^{-1}$ range with a Beckman IR 4200 spectrophotometer. The DTA scans were recorded to determine the glass transition and crystallization temperatures using a Shimadzu DTA-50H machine. The phases precipitated in glassy matrix during different heat treatment schedules, were examined by X-ray diffraction using a computerized Rich-Seifert ID-3000 X-ray diffractometer with nickle filtered $\text{CuK}\alpha$ radiation. Polished surfaces were prepared using various SiC and diamond polishing compounds. Finally polishing was done with a 0.25 micron diamond paste for an optical finish. Polished samples were etched using solution containing 2% HF and 5% HCl for 30 sec. Charging problems were circumvented in SEM examination by the deposition of a thin layer (20 to 50 nm) of Au-Pd film sputtered onto the specimen surface. Polished and etched surfaces of polycrystalline specimens were observed by SEM (Model PSEM 500). The dielectric constant and loss factor of different glass ceramics were measured using an HP 4192A LF impedance analyzer from 100 Hz to 1 MHz and in the temperature range 300–500 K. Silver paint (Code No. 1337-A Elteck Corporation) was applied on both sides of the specimen and was cured at 973 K for 5 min.

3. Results and discussion

The compositions of base glass and glass containing CoO are given in table 1. The crystallization and other characteristics of glass no. 1 are reported earlier (Thakur *et al* 1995a). In this paper we are also representing some data for glass no. 1 for the sake of comparison. The infrared spectra for the glasses 1 and 2 are shown in figure 1. IR spectra of these glasses generally consisted of broad and diffuse bands in the region $400\text{--}1400\text{ cm}^{-1}$. Each broad peak might be showing the one or more vibration contributions from group of ions. B_2O_3 gives an intense band in the range of $1200\text{--}1400\text{ cm}^{-1}$ which involves the vibration of a B–O–B bond constituting the

Table 1. Composition of various glasses (wt%).

Batch name	(SrO·TiO ₂)	(2SiO ₂ ·B ₂ O ₃)	CoO
Glass 1	65	35	0
Glass 2	64	35	1

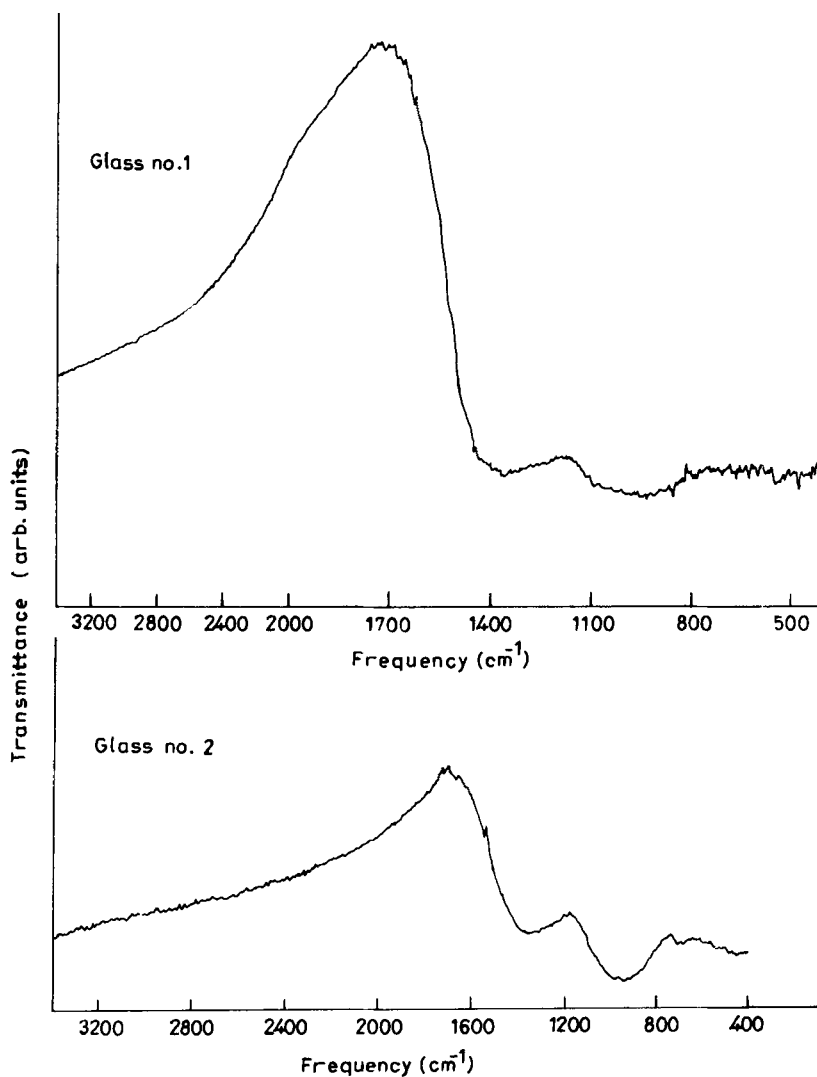


Figure 1. Infrared spectra of glasses 1 and 2.

linkage of boroxol group to neighbouring groups. This band also corresponds to the bond stretching vibration of the boron sublattice against the oxygen sublattice (Krogh-Moe 1965). The second absorption peak at $900\text{--}1000\text{ cm}^{-1}$ may be assigned to a 'bond stretching' vibration of Si-O-Si in which the bridging oxygen atoms move in the opposite direction to their Si neighbours and are highly parallel to the Si-O-Si lines. Other vibrations involving the motion of the B-O-Si linkages in the borosilicate structure and BO_4 tetrahedras may also give absorption in this range. The band in the region of $900\text{--}1000\text{ cm}^{-1}$ appears broad for base glass (glass no. 1) which undoubtedly consists of several absorption peaks and results in the disorder of the glass network. The increase in the intensity of absorption band at $900\text{--}1000\text{ cm}^{-1}$ for glass no. 2 can be correlated with the creation of non-bridging oxygens of weaker bonding strength.

The weaker bands at 720 cm^{-1} and around 500 cm^{-1} for glass no. 2 arise from bond bending and rocking motion of the B–O–B linkages within the glassy network (Krogh-Moe 1965). The absorption peak at 720 cm^{-1} for glass no. 2 may also be attributed to a 'bending rock' perpendicular to the Si–O–Si planes. No essential changes could be observed in the infrared spectra of base glass nos 1 and 2 containing 1 wt% CoO. The only difference being that the absorption peak intensity increases at $900\text{--}1000\text{ cm}^{-1}$ for the glass containing CoO.

The DTA plots for glasses 1 and 2 are shown in figure 2. The DTA pattern for base glass 1 shows that the glass transition temperature is around 700°C and an exothermic peak at about 947°C which is ascribed to crystallization temperature. This exothermic peak may be assigned to the crystallization of rutile as principal phase followed by $\text{Sr}_2\text{B}_2\text{O}_5$ and $\text{Sr}_3\text{Ti}_2\text{O}_7$ phases (Thakur *et al* 1995a). Cobalt oxide addition in base glass contributes in lowering the glass transition temperature which appears around 680°C . Two crystallization peaks appear for the glass containing 1 wt% CoO. The first exothermic peak around 860°C is due to the crystallization of rutile, $\text{Sr}_2\text{B}_2\text{O}_5$ and $\text{Sr}_3\text{Ti}_2\text{O}_7$ phases while second peak at 935°C may be attributed to the crystallization of $\text{SrB}_2\text{Si}_2\text{O}_8$, $\text{Sr}_3\text{B}_2\text{SiO}_8$ and some unidentified phases. The second crystallization peak

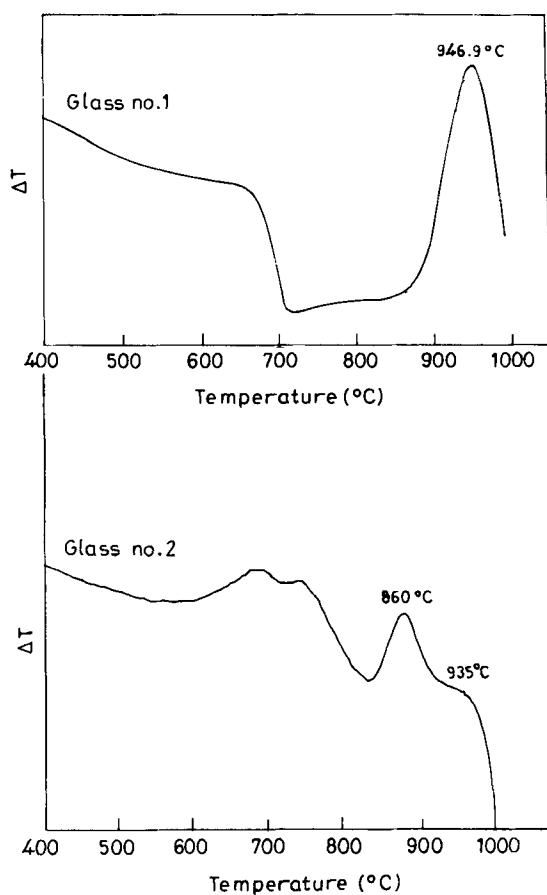
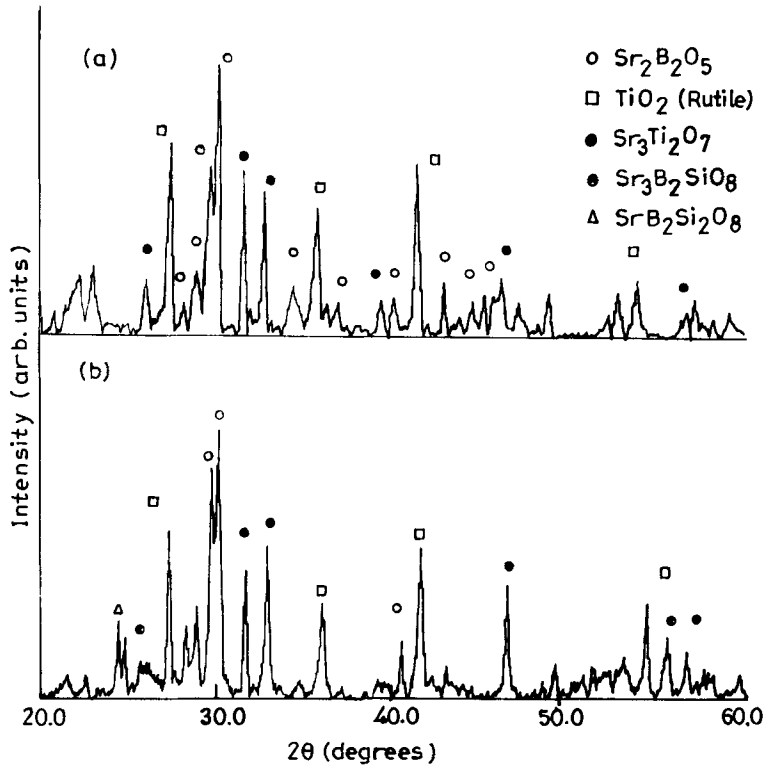


Figure 2. DTA plots for glasses 1 and 2.

Table 2. Different peaks observed in DTA study.

Batch	T_g	T_{c_1}	T_{c_2}
Glass 1	692 C	947 C	-
Glass 2	685 C	860 C	935 C

**Figure 3.** XRD patterns for glass 2 crystallized at (a) 900 °C/3 h and (b) 950 °C/3 h.

occurred over a wide temperature range than that of first exothermic peak which indicates the crystallization of some more phases. Table 2 illustrates the glass transition and crystallization temperatures for glasses 1 and 2.

All the glasses subjected to different heat treatment schedules were heated to 500°C for 1 h prior to crystallization. When base glass was heat treated at 900°C for 3 h, it resulted in the crystallization of rutile phase in a major amount with some unknown phase. If the heating rate for crystallization was made little slower (2°C/min) with longer duration (12 h) of holding time at growth temperature, $Sr_2B_2O_5$ and $Sr_3Ti_2O_7$ also started growing along with rutile phase. Strontium borate appears as major phase accompanied by rutile and $Sr_3Ti_2O_7$. With further increment in crystallization temperature (950°C for 3 h) the rutile phase constitutes as the principal phase with $Sr_2B_2O_5$ and $Sr_3Ti_2O_7$. From this study, one can infer that the rutile phase starts precipitating quite faster than other phases viz. $Sr_2B_2O_5$, $Sr_3Ti_2O_7$ etc. It is observed that the growth of $Sr_2B_2O_5$, $Sr_3Ti_2O_7$ are conducive to either higher crystallization

temperature or longer duration of holding at low crystallization temperature (Thakur *et al* 1995a). XRD patterns of glass ceramics containing 1 wt% CoO, crystallized for 3 h at 900°C and 950°C are presented in figures 3a and b respectively. As discussed in DTA study, addition of 1 wt% CoO in the base glass does lower the glass transition and crystallization temperatures. When this glass sample is heat treated at 900°C for 3 h, crystallization of $\text{Sr}_2\text{B}_2\text{O}_5$ occurs with $\text{Sr}_3\text{Ti}_2\text{O}_7$ and rutile as minor phase. In this case, strontium borate appears as the major crystalline phase in contrast to base glass ceramic where rutile phase was present in major amount for the same heat treatment schedule. There is no major change observed for the glass ceramic crystallized at 950°C for 3 h. This also shows similar phase constitution as to that of base glass crystallized at 900°C for 3 h. Only difference is $\text{SrB}_2\text{Si}_2\text{O}_8$ and $\text{Sr}_3\text{B}_2\text{SiO}_8$ also start crystallizing at 950°C.

Figure 4a shows the SEM micrograph for base glass ceramic crystallized at 900°C for 12 h. The microstructure of glass ceramic mainly consists of acicular, needle-like and spherical crystallites of $\text{Sr}_2\text{B}_2\text{O}_5$, TiO_2 (rutile), $\text{Sr}_3\text{Ti}_2\text{O}_7$ respectively. As it is clear from the micrograph that the crystallite size of $\text{Sr}_2\text{B}_2\text{O}_5$ ($\geq 1 \mu\text{m}$) is larger than the other phases. These crystallites are well connected with each other. $\text{Sr}_3\text{Ti}_2\text{O}_7$ (spherulites) starts appearing around the $\text{Sr}_2\text{B}_2\text{O}_5$ phase. At higher temperature (950°C), growth of rutile crystal retards while $\text{Sr}_2\text{B}_2\text{O}_5$ and $\text{Sr}_3\text{Ti}_2\text{O}_7$ begin to grow rapidly. Figures 4b and c depict the micrographs for glass ceramic specimen containing 1 wt% CoO crystallized at 900°C and 950°C for 3 h, respectively. These microstructures are in conformity with the results of XRD and indicate similar phase progression. Figure 4b exhibits the crystallites of $\text{Sr}_2\text{B}_2\text{O}_5$, rutile and $\text{Sr}_3\text{Ti}_2\text{O}_7$ etc. Growth of strontium borate occurs in one dimension. Fine crystals of $\text{Sr}_3\text{Ti}_2\text{O}_7$ are present which are surrounded by $\text{Sr}_2\text{B}_2\text{O}_5$ phase. When the temperature for this glass ceramic is raised to 950°C, fine crystals of all the phases in the submicron size were observed. Spherical crystals of $\text{Sr}_3\text{Ti}_2\text{O}_7$ segregated among strontium borate crystallites and can be clearly seen from figure 4c. Crystallization of these three phases occurs simultaneously at higher temperature so that there is a competition for SrO between $\text{Sr}_2\text{B}_2\text{O}_5$, $\text{Sr}_3\text{Ti}_2\text{O}_7$, $\text{SrB}_2\text{Si}_2\text{O}_8$ and $\text{Sr}_3\text{B}_2\text{SiO}_8$ phases which result in fine microstructure of resulting glass ceramics.

The detailed investigations into the dielectric behaviour of base glass ceramics have been published elsewhere (Thakur *et al* 1995a). Figure 5 shows the variation of dielectric constant and dissipation factor with temperature for glass no. 2. The values of dielectric constant and dissipation factor fall in the range 10–20 and 0.07–0.15 respectively. Variation of dielectric behaviour is almost independent with temperature. It is interesting to note that the dielectric behaviour of glass ceramic containing 1 wt% CoO, crystallized at 900°C for 3 h shows similar trend to that of parent glass. Only the values of dissipation factor were found to be lower than that of parent glass due to presence of low conductive crystalline phases. Dielectric constant varies very little up to a particular temperature then rises very fast owing to space charge polarization. Dielectric constant and dissipation factor depend on frequency. Dielectric constant decreases with increasing frequency. A maxima is observed in the variation of dissipation factor with respect to frequency. This behaviour may be attributed to relaxation of space charge polarization. Hence, there is a different type of variation in dissipation factor with respect to temperature above and below the frequency of maxima (100 KHz). At low frequency, it decreases with temperature while it increases with temperature at higher frequency. Figure 6 illustrates the temperature variation of dielectric constant and dissipation factor for glass ceramic crystallized at 950°C for 3 h.

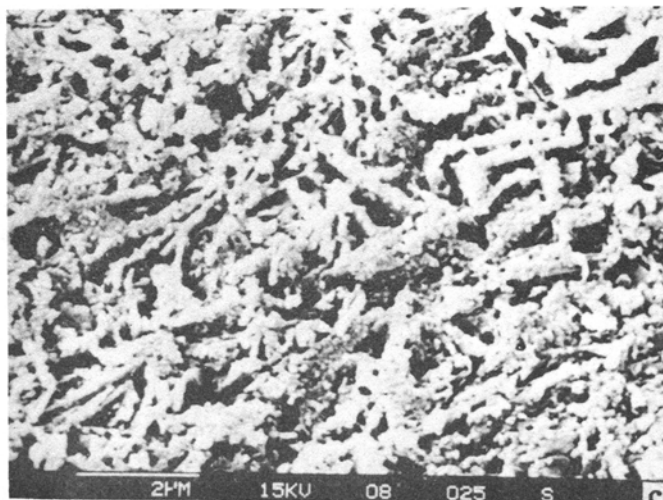
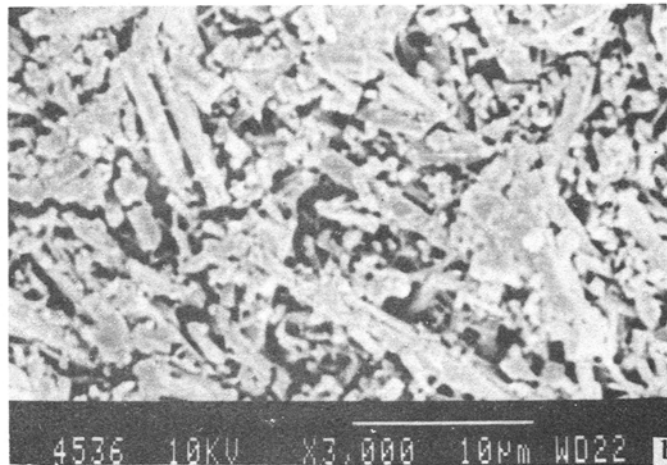
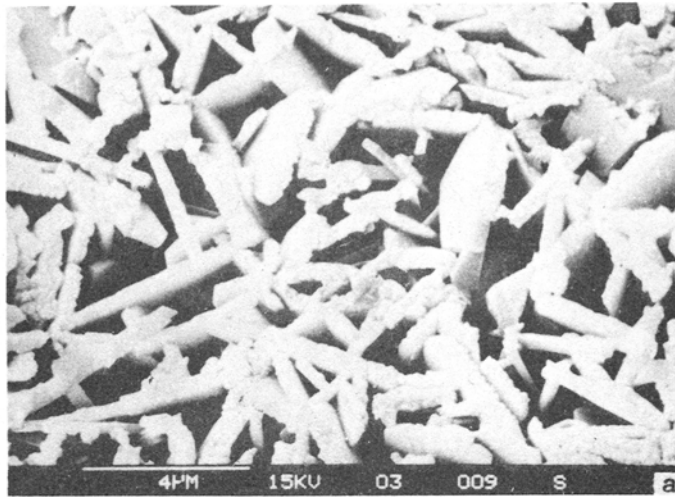


Figure 4. Scanning electron micrographs of (a) glass 1 crystallized at 900°C for 12 h, (b) glass 2 crystallized at 900°C for 3 h and (c) glass 2 crystallized at 950°C for 3 h.

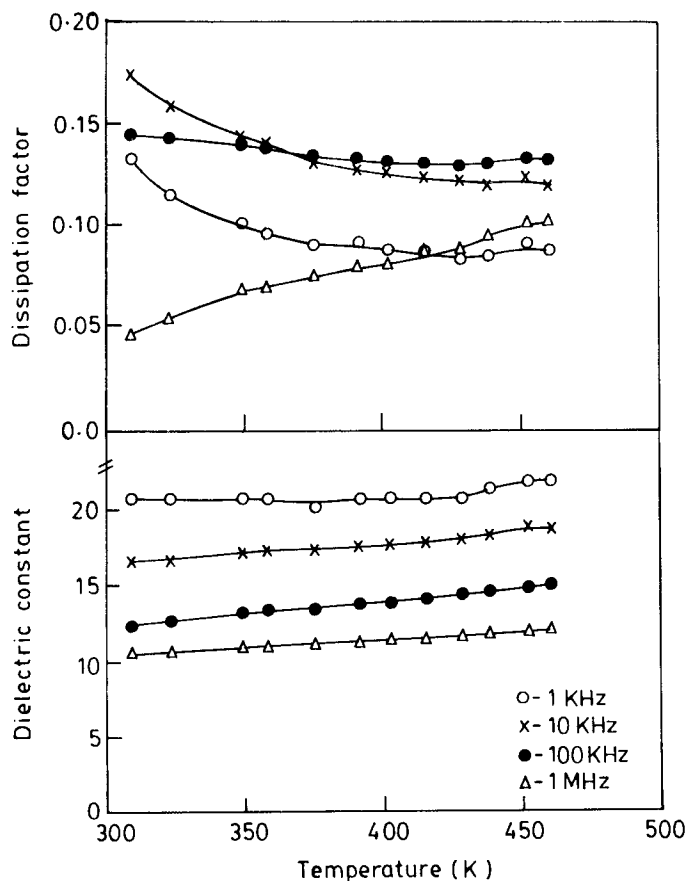


Figure 5. Variation of dissipation factor and dielectric constant with temperature of glass 2.

It shows very little or no variation in dielectric behaviour. This can be understood in terms of very fine crystallite size clamped rigidly in glassy matrix. The dissipation factor decreases slightly with temperature. But more or less the trend is similar to that of temperature variation of dielectric constant. The values of dielectric constant, dissipation factor, density, corresponding crystalline phases and temperature coefficient of capacitance (TCC) for different glass and glass ceramic samples are given in table 3.

The observed dielectric characteristics of various glass ceramics can be interpreted on the basis of their respective micrographs. Micrographs of the specimens which depict the uniform distribution of fine crystallites in glassy matrix may cause meagre variation in dielectric characteristics up to very high temperature. However, samples with irregular size of crystallites show appreciable change in dielectric behaviour with temperature and frequency. The higher thermal stability and lower dielectric loss of CoO containing glass ceramic may be attributed to charge compensation of defects responsible for dielectric loss. These glass ceramics also contain $\text{Sr}_2\text{B}_2\text{O}_5$ as major phase and TiO_2 as minor phase.

In certain circumstances, the grain or grain boundary resistance dominates the overall impedance. A single semicircle is then seen in the complex impedance plots. If the same data are reproduced and presented in the complex electric modulus, M^* ,

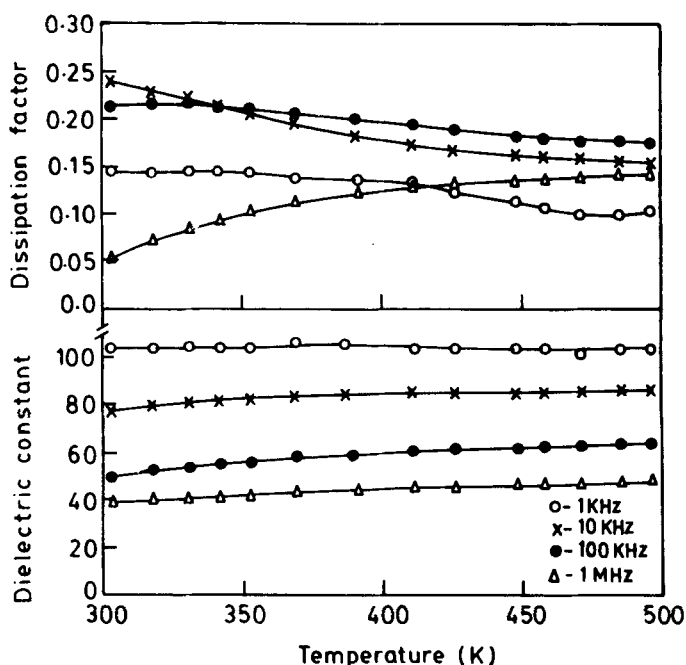


Figure 6. Variation of dissipation factor and dielectric constant with temperature of glass 2 crystallized at 950°C for 3 h.

Table 3. Characteristics of glasses and glass ceramic samples.

Batch name	Heat treatment parameters			Phases observed (XRD)	Density (g/cm ³)	Dielectric parameters at room temperature and 1 KHz		
	Temp. (°C)	Heating rate (°C/min)	Holding time (h)			ϵ'	$\tan \delta$	TCC $\times 10^3$ ppm/K
Glass 1	--	--	--	--	3.84	60	0.27	1.923
Glass 2	--	--	--	--	3.26	21	0.07	0.379
Glass 1	905	15	48	SB + ST + R	4.03	40	0.02	0.168
Glass 1	950	05	03	SB + R + ST	4.01	100	0.20	0.636
Glass 2	900	05	03	SB + R + ST	3.40	100	0.15	0.554
Glass 2	950	05	03	SB + R + ST SS + SS2	3.40	20	0.015	-0.142

(XRD phases are abbreviated as: SB = Sr₂B₂O₅; ST = Sr₃Ti₂O₇; R = TiO₂; SS = Sr₃B₂SiO₈; SS2 = SrB₂Si₂O₈)

formalism then the response of both grain boundary and bulk regions may be seen. The complex plane electric modulus plots are shown in figures 7 and 8 as a function of temperature for 1 wt% CoO containing glass and glass ceramic (heat treated at 950°C for 3 h) respectively. These show two poorly resolved semicircles. Figures 9a and b illustrate spectroscopic plots of the imaginary component M'' at different temperatures for glass and glass ceramic containing 1 wt% CoO crystallized at 950°C for 3 h. Values of capacitance increases with increasing temperature. The broad peak in the

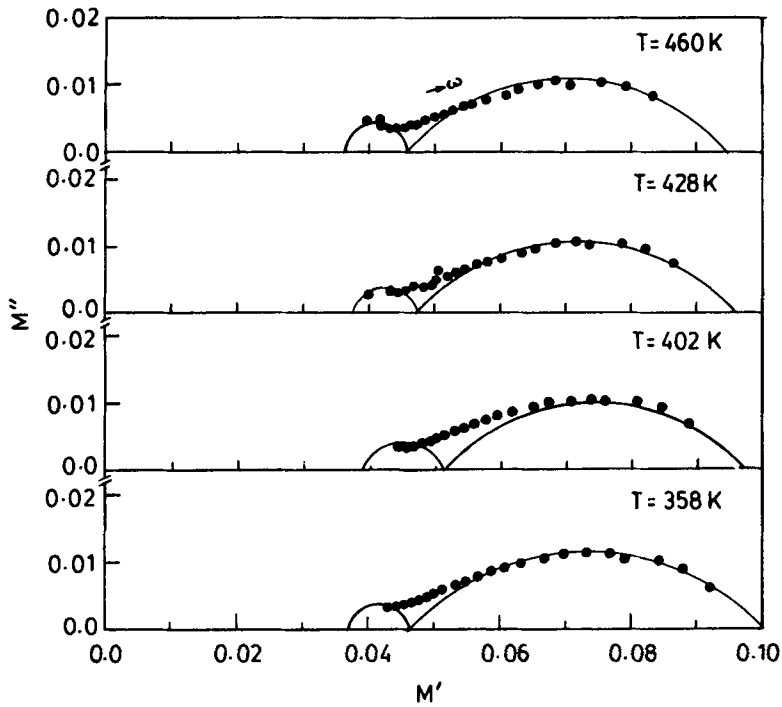


Figure 7. Complex electric modulus plots for glass 2 at different temperatures.

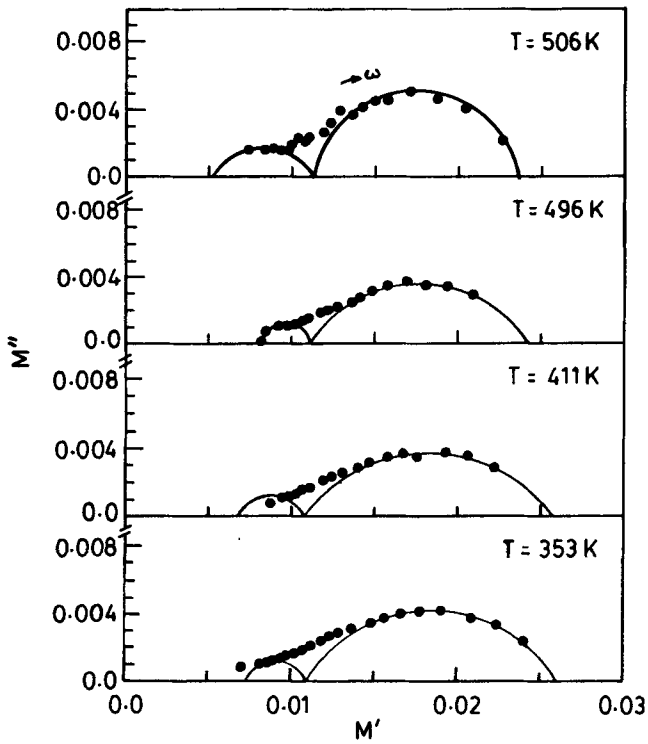


Figure 8. Complex electric modulus plots for glass 2 crystallized at 950°C for 3 h at different temperatures.

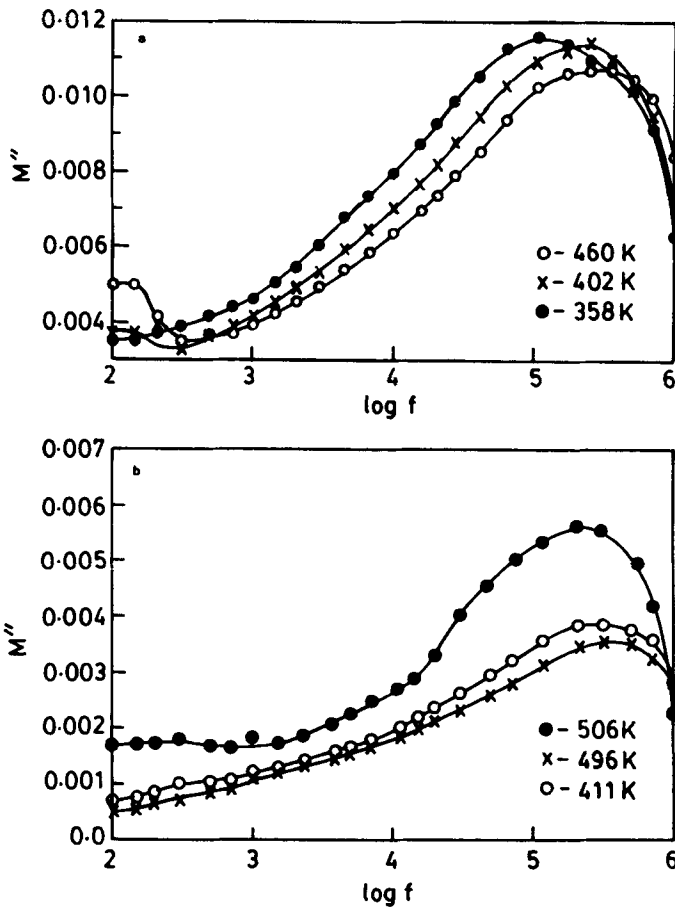


Figure 9. Spectroscopic plot of imaginary modulus component (M'') for (a) glass 2 and (b) glass 2 crystallized at 950°C for 3 h at different temperatures.

modulus spectrum can be assigned either to a summation of relaxations occurring within the bulk material or the presence of phases of more than one composition or structure. This peak may be resolved into two peaks which may correspond to an equivalent circuit with two RC elements in series, approximately equal in C but differing in R . The higher frequency M'' peak represents a bulk component of the sample. Modulus plots pick out these elements with the smallest capacitance since the M'' peak maximum is equal to $\epsilon_0/2C$ for that particular element.

4. Conclusions

The present studies indicate that the 1 wt% CoO in base glass imparts prominently the following properties: (i) lowers the glass transition temperature and crystallization temperatures, (ii) render temperature independent behaviour to dielectric characteristics, and (iii) strontium borate appears as the principal phase followed by rutile and $\text{Sr}_3\text{Ti}_2\text{O}_7$ phase. $\text{SrB}_2\text{Si}_2\text{O}_8$ and $\text{Sr}_3\text{B}_2\text{SiO}_8$ start crystallizing at higher temperature (950°C). From the present investigation and earlier work we find that due to competition

of SrO among different crystalline phases it is difficult to crystallize SrTiO₃ phase in these glass ceramics similar to the case of aluminosilicate glass ceramics. But these glass ceramics also show better thermal stability and may be used for similar applications as described for SrTiO₃ glass ceramics.

Our subsequent effort has shown that by suitably adding K₂O we can easily crystallize SrTiO₃ phase in borosilicate glass ceramics (Thakur *et al* 1995b).

Acknowledgements

One of the authors (OPT) is highly thankful to the Department of Atomic Energy, Bombay for a research fellowship. Partial financial support from UGC and CSIR is gratefully acknowledged.

References

- Bergeron C G and Russell C K 1965 *J. Am. Ceram. Soc.* **48** 115
Borelli N F 1967 *J. Appl. Phys.* **38** 4243
Hirayama C and Subbarao E C 1962 *Phys. Chem. Glasses* **3** 111
Krogh-Moe J 1965 *Phys. Chem. Glasses* **6** 46
Lawless W N 1971 *Adv. Cryogenic Engg.* **16** 261
Lawless W N 1974 *Ferroelectrics* **7** 379
Lynch S M and Shelby J M 1984 *J. Am. Ceram. Soc.* **67** 42
McMillan P W 1979 *Glass ceramics* (London: Academic Press) 2nd ed.
Mel' nichchenko L G 1970 *Steklo j. Keram.* **27** 22
Orlova E S 1969 *Steklo Trudy Inst. Stekla* **2** 68
Swartz S L 1985 *Dielectric properties of strontium titanate glass ceramics*, Ph D Thesis, The Pennsylvania State University, USA
Swartz S L and Bhalla A S 1986 *Mater. Res. Bull.* **21** 1417
Swartz S L, Brevel E and Bhalla A S 1988 *Am. Ceram. Soc. Bull.* **67** 763
Thakur O P, Devendra Kumar, Parkash Om and Pandey L 1993 *Proc. national symposium on high-tech ceramics, Varanasi* 70
Thakur O P, Devendra Kumar, Parkash Om and Pandey L 1995a *Bull. Mater. Sci.* **18** 577
Thakur O P, Devendra Kumar, Parkash Om and Pandey L 1995b *Mater. Lett.* **23** 253